# Supporting Information

# Biological Degradation of Graphitic Carbon Nitride Sheets and Autophagy Induction in Macrophages

*K. Swetha[a], Anushree Bhatnagar[b], Manikrishna Lakavathu[a], Penta Poornima[c], Pratiksha Ganesh[a], Adithi Kamath[a], Srinivasa Reddy Bonam[c], Srinivasa M. Srinivasula[b] and Rajendra Kurapati*[a,d]*

[a] *School of Chemistry, Indian Institute of Science Education and Research Thiruvananthapuram, Maruthamala P.O., Vithura, Thiruvananthapuram, Kerala 695551, India. E-mail: rkurapati@iisertvm.ac.in*

[b] *School of Biology, Indian Institute of Science Education and Research Thiruvananthapuram, Maruthamala PO, Vithura, Thiruvananthapuram 695551, Kerala, India.*

[c] *Department of Natural Products and Medicinal Chemistry, CSIR-Indian Institute of Chemical Technology (IICT), Hyderabad 500007, Telangana, India.*

[d] *The Centre for Advanced Materials Research with International Engagement, (CAMRIE), Indian Institute of Science Education and Research Thiruvananthapuram, Maruthamala P.O., Vithura, Thiruvananthapuram, Kerala 695551, India.*

## Materials and Methods

**Synthesis of exfoliated (Exf) ultrathin g-$C_3N_4$ sheets**

Exfoliated ultra-thin g-$C_3N_4$ nanosheets were prepared following the work of Zhang et al.[1] First, 0.1 g of bulk g-$C_3N_4$ in 100 mL distilled water was sonicated for 16 hr, where the water temperature was kept below room temperature by adding ice. The resulting suspension was centrifuged at 5000 rpm for 10 min to remove unexfoliated bulk g-$C_3N_4$. The supernatant suspension was filtered using Whatman vacuum filtration (0.2 µm). Finally, the Exf g-$C_3N_4$ nanosheets were collected and characterized further.

**Synthesis of porous (Por) g-$C_3N_4$**

Por g-$C_3N_4$ was synthesized by the chemical oxidation of commercially purchased bulk g-$C_3N_4$ using $K_2Cr_2O_7$ following the previous report.[2] First, a mixture of 4 g of $K_2Cr_2O_7$ was taken in 20 mL $H_2SO_4$ and stirred for 10 min until the solution turned brown. This mixture added 0.2 g of bulk g-C3N4 and stirred further for 2 hr at RT. Next, the mixture was poured into 160 mL of deionized water and cooled to RT. This solution was centrifuged at 6000 rpm for 10 min to obtain a light-yellow precipitate. The precipitate was further dialyzed to remove all the acid, and a milk-white suspension was obtained. Later, the suspension was dispersed in water and sonicated for 2 hr. The obtained suspension was centrifuged at 3000 rpm for 5 min to remove the undispersed g-$C_3N_4$. The supernatant solution was lyophilized to obtain the Por g-$C_3N_4$ powder.

**Enzymatic degradation of exfoliated and porous g-$C_3N_4$ by hMPO**

Biodegradation of Exf and Por g-$C_3N_4$ sheets was performed by treating them with hMPO in the presence of $H_2O_2$ and NaCl with minor modifications.[3] In brief, 0.02 mg Exf or Por g-$C_3N_4$ was resuspended in 125 µL of 50 mM PBS (including 140 mM NaCl and 100 µM DTPA). Next, 12.5 µL of 100 ug/µL of hMPO was added to the reaction mixture, followed by the addition of 1 µL of 200 µM $H_2O_2$ per hour for 60 hr in total. hMPO was renewed every 5 hr. The reaction was carried out in a 37 °C incubator. The control samples were also prepared without adding hMPO. Since hMPO is light-sensitive, the experimental samples were covered with aluminium foils. The aliquots (10 µL) were collected at 0, 20, 40 and 60 hr and stored at -20℃ for further characterisation.

**Enzymatic degradation of exfoliated and porous g-$C_3N_4$ by HRP**

The biodegradation of Exf and Por g-$C_3N_4$ sheets by the plant peroxidase (HRP) was performed similarly to the previous report.[4] Briefly, 0.1428 mg/mL of Exf or Por g-$C_3N_4$ was prepared in phosphate buffer saline (PBS). Further, the mixture was sonicated for 2 min, and then 0.1714 mg/mL of HRP was added. Next, 1.57 µL of 142 µM of $H_2O_2$ was added every 24 hr for 60 days. Also, HRP was renewed every 20 days due to loss of enzymatic activity after 20 days. HRP was not added for the control samples, while 142 µM of H2O2 was added daily for up to 60 days. The reaction was conducted in dark conditions to avoid light interaction with the samples. The aliquots (30 µL) were collected on 0, 20, 40 and 60 days and stored at -20°C for further characterization.

**Degradation of g-$C_3N_4$ by UV-catalysed Photo-Fenton reaction**

Degradation of g-$C_3N_4$ under UV-catalysed Photo-Fenton reaction was performed as reported earlier.[14] In brief, the g-$C_3N_4$ stock solution was prepared by resuspending 0.546 mg of g-$C_3N_4$ in 2.46 mL water adjusted to pH 4 using 0.1 M HCl. Next, 10 µL of 1 mM $FeCl_3.H_2O$ was added every 35 hr and 100 µL of 50mM $H_2O_2$ was added every 10 hr up to 150 hr. The reaction was carried out with a UV lamp operating at 100 W and a ballasted lamp at 365 nm. The reaction was carried out in quartz tubes kept around 6 cm away from the UV lamp. The sample was initially sonicated for 5 minutes and then further sonicated every 10 hr to prevent agglomeration. 200 µL sample aliquots were collected at 0 hr, 50 hr, 100 hr, and 150 hr and stored at -20℃ for further characterization.

**Characterization of g-$C_3N_4$**

The synthesized Por g-$C_3N_4$ and Exf g-$C_3N_4$ nanosheets were characterised by UV-visible spectroscopy, Raman spectroscopy, fluorescence spectroscopy and transmission electron spectroscopy (TEM).

**Zeta Potential and Dynamic Light Scattering**

The zeta potential of the samples was analyzed using the Malvern Zeta-sizer Nano ZS instrument fitted with a laser of 655 nm. The samples were well dispersed in the Milli-Q water by sonication, and the zeta potential of the samples was measured using an electrophoretic cell. The average of three measurements was used for analysis.

**High-resolution TEM (HRTEM)**

First, 6 µL of samples were sonicated for 5 minutes and drop cast on carbon-coated copper grids. It was dried under IR irradiation. The salts in the samples due to the PBS buffer were removed by washing with Milli Q water for 20 minutes and then drying them under an IR lamp. FEI TECHNAI G2 F30 S-Twin, operating at 300kV, was used for high-resolution TEM (HRTEM) imaging.

**Raman Spectroscopy Analyses**

Raman samples were prepared by drop casting 6 µL of samples post-sonication on a clean glass slide. It was dried under an IR Lamp. Analysis was done with Lab RAM HR Raman Optical Spectrometer equipped with a 633 nm laser and a Leica microscope. The spectra were recorded using a 100X objective lens and 3% laser power for both Exf and Por g-C3N4 samples. For Exf g-$C_3N_4$ nanosheets, a D2 filter was used, whereas no filter was used for Por g-$C_3N_4$. The spectra were plotted in Origin Lab software with an average of 5 spectra taken into consideration to account for the non-uniform degradation. All the graphs were baseline corrected with 10-point baseline correction subtracted from the baseline dataset.

**Fluorescence spectroscopy**

The photoluminescence spectra were recorded on a spectrofluorometer (Horiba Jobin Yvon- Fluorolog 3). The samples were dispersed in DI water at 0.1 mg/mL for all the fluorescence studies. Measurement was done in FluoroEssence V38 software.

**X-ray Diffraction Pattern (XRD)**

The powder X-ray diffraction analyses of bulk, Exf, and Por samples were analyzed using the Panalytical powder XRD instrument (CuKα) with parameters 40 mA, 40 kV, and λ = 1.5406 Å. The 2θ values were analyzed in the 5-80° range with a scan rate of 1.8° per min. The data was analyzed and plotted using Origin software.

**UV-visible Spectroscopy**

A quartz cuvette of 1 mm path length was used to measure the absorption peak. The spectra were recorded using a Shimadzu UV-3600 Vis-NIR spectrophotometer. Milli Q was used to take the baseline reading. The spectral data was analyzed and plotted in Origin Lab software.

**Atomic Force Microscopy (AFM)**

AFM samples were prepared on a clean and dried glass slide, where 6 µL of the samples were drop casted post-sonication and dried under an IR lamp. JPK Nanowizard 4AFM was used to analyze the samples with a scale range of 10 x 10 µm. The surface roughness and height of the sample were interpreted using JPK software.

**X-ray photoelectron spectroscopy (XPS)**

First, 6 µL of 0 hr and 150 hr g-$C_3N_4$ samples were drop cast on freshly cleaned silicon wafers, which were dried using IR irradiation for 15 min. To obtain a thicker coating, samples were drop casted and dried 5 times. XPS analysis was performed using Omicron Nanotechnology XPS. The XPS spectra were analyzed using the software Casa-XPS.

**Low-Resolution Mass Spectrometry (LRMS) Analyses**

The samples degraded by UV-light catalysed photo Fenton reaction were analyzed using low-resolution mass spectrometry. The protocol followed for mass spectrometry is as reported earlier.[5, 6]. The sample was diluted in acetonitrile in a 1:5 (v/v) ratio and measured using Thermoscientific Q Benchtop LRMS. The sample was infused into the ESI source at 3 µL/min. The common fragmentation channels correspond to multiple losses and gains of amine (16 Da), hydroxyl (17 Da), carboxylic acid (45 Da), aldehyde (29 Da) and cyanamide groups (42 Da) were applied for identifying the degradation products. The data was plotted using Origin Lab software.

**Cytotoxicity and autophagy studies of exfoliated and porous g-$C_3N_4$**

RAW 264.7 macrophage cells were transfected with pmRFP-LC3 plasmid using lipofectamine 3000 as per the manufacturer's instructions and grown on coverslips (The RAW264.7 macrophage cells were procured from ATCC and maintained in the tissue culture facility of Prof. S. Murty Srinivasula's laboratory. The RAW GFP-LC3 cell line was generated by Prof. S. Murty Srinivasula's group in RAW264.7 cells by stably expressing GFP-LC3 using pMYs-IRES-GFP as reported previously by Fujita et al., 2011).

RAW 264.7 cells overexpressing mRFP-LC3 were incubated with the indicated concentrations of Exf or Por g-$C_3N_4$. Cells growing on coverslips were fixed using 4% paraformaldehyde after 6, 12 and 24 hr of incubations. Cells were imaged using an Olympus FV3000 laser scanning microscope at 60X. Images used for representation were intensity-adjusted and processed using ImageJ software. Z-stack images were acquired by keeping a constant slice size of 0.38 µm. To identify GFP-LC3 bands, RAW GFP-LC3 macrophages were incubated with Exf or Por g-$C_3N_4$ for the indicated durations. Cells were collected after incubation and mixed with Laemmli buffer and boiled. Protein samples were resolved on SDS–PAGE followed by Western transfer to PVDF membranes (IPVH00010, Merck) at 90V. Anti-GFP (sc-9996, Santa Cruz Biotechnology) and anti-α-tubulin (12G10, DSHB) antibodies were used to probe the membranes. The signals were visualized using a chemiluminescent HRP substrate (RPN2236, Cytiva) on the ChemiDoc XRS+ imaging system using QuantityOne software. Primary antibodies were used at 1:1000 dilutions and secondary antibodies were used at 1:5000 dilutions.

Cytotoxicity test was performed by culturing RAW 264.7 macrophage cells in DMEM culture media with 10% fetal bovine serum (FBS) and 1% penicillin & streptomycin antibiotic added, in a 96-well plate for 24 hr in an incubator maintaining 37 °C and a 5% CO2 level. Next, cells were treated with g-$C_3N_4$ and incubated for 24 h, followed by washing with PBS once, and then, MTT (Sigma Aldrich) diluted with media was added to the cells and incubated for 3-4 hr in a $CO_2$ incubator at 37°C. Crystals formed were dissolved in molecular grade DMSO. Absorbance was taken using a microplate reader at 570nm. Subsequent plots were drawn to interpret the results as shown.

**Cytokine studies of exfoliated and porous g-$C_3N_4$**

RAW 264.7 cells (RAW 264.7 macrophage cells are a kind gift from the tissue culture facility, CSIR-CCMB, Hyderabad, India) were grown in High Glucose Dulbecco's Modified Eagle Medium (HDMEM) supplemented with 10% FBS, 100 u/mL penicillin and 0.1 mg/mL streptomycin with 5% $CO_2$ incubator at 37°C. Macrophages were seeded in 12 well plates at a density of $5\times10^5$ cells/well and incubated for 24 hr. Cells were then incubated with different concentrations of either exfoliated or porous nanosheets for 24 hr by taking the LPS (100 ng/mL) as standard, and the supernatant was collected for assessing the immunomodulatory activity. Nitric oxide assay was performed using Griess reagent. A 100 µL of Griess reagent was added to 100 µL of each sample and incubated for 20 minutes in the dark. Absorbance was measured at 545 nm by using a microplate reader. The Sandwich ELISA method was performed as reported earlier, to estimate the cytokine production.[7, 8] Cytokines ELISA kits are purchased from BD Biosciences.

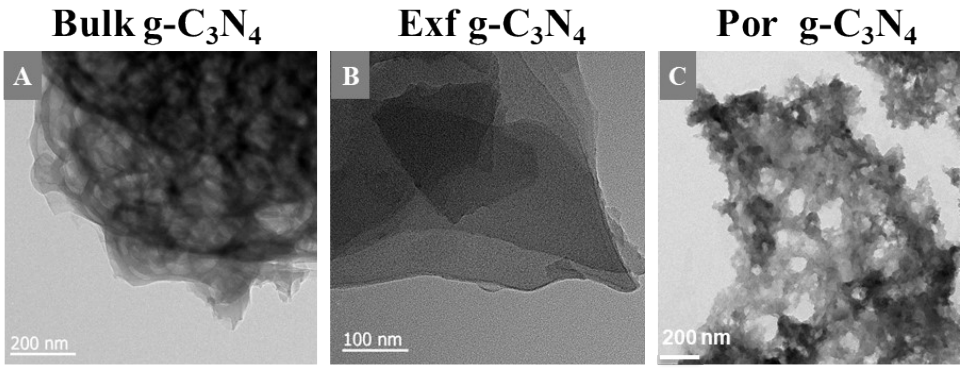


**Figure S1:** TEM images of bulk (A), Exf (B) and Por (C) g-$C_3N_4$ nanosheets, respectively.

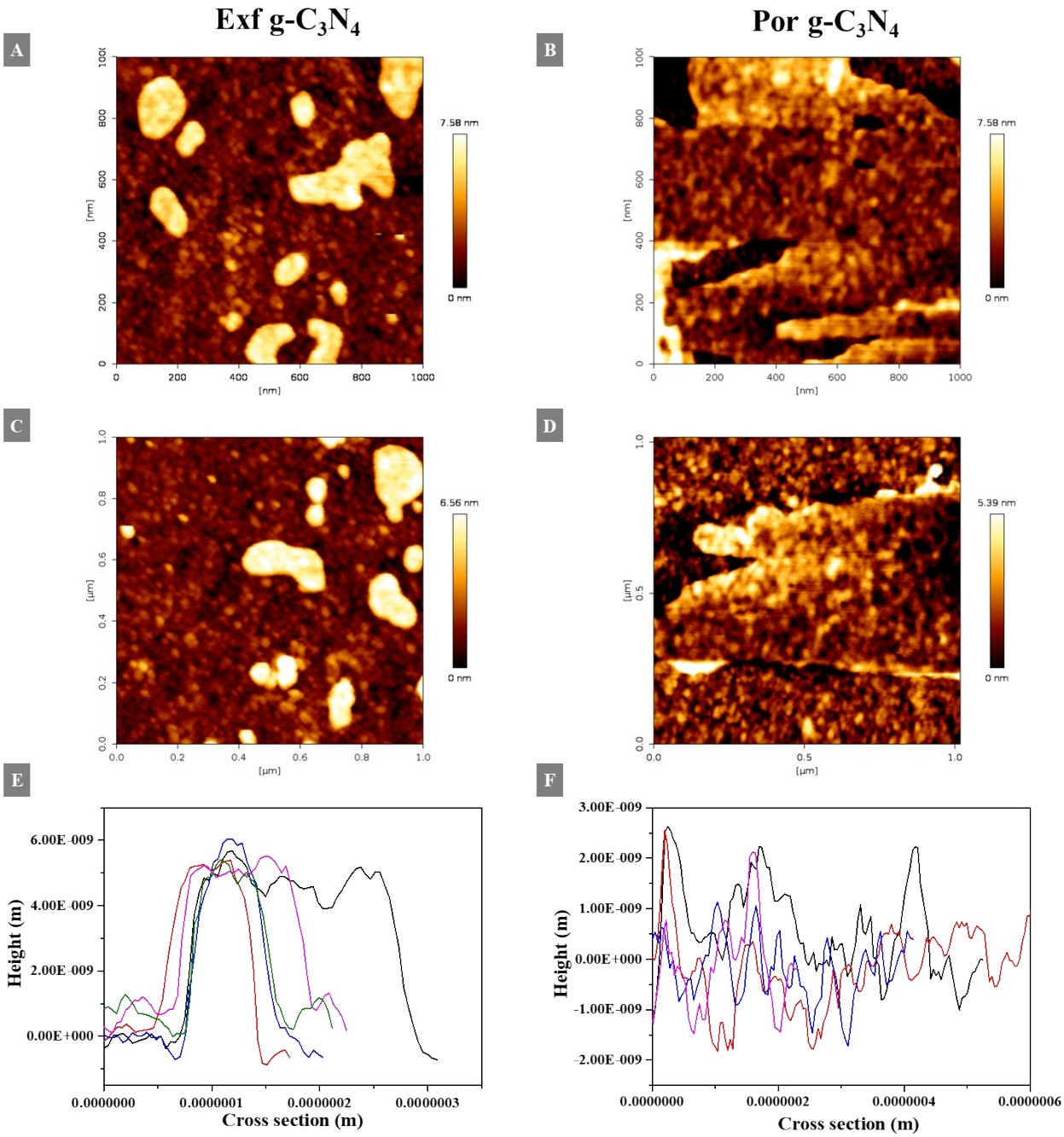


**Figure S2:** AFM images of the synthesized Exf and Por g-$C_3N_4$ nanosheets along with corresponding height profiles of random nanosheets showing the thin sheet morphology Exf g-$C_3N_4$ (E) and porous structure of Por g-$C_3N_4$ nanosheets (F), respectively.

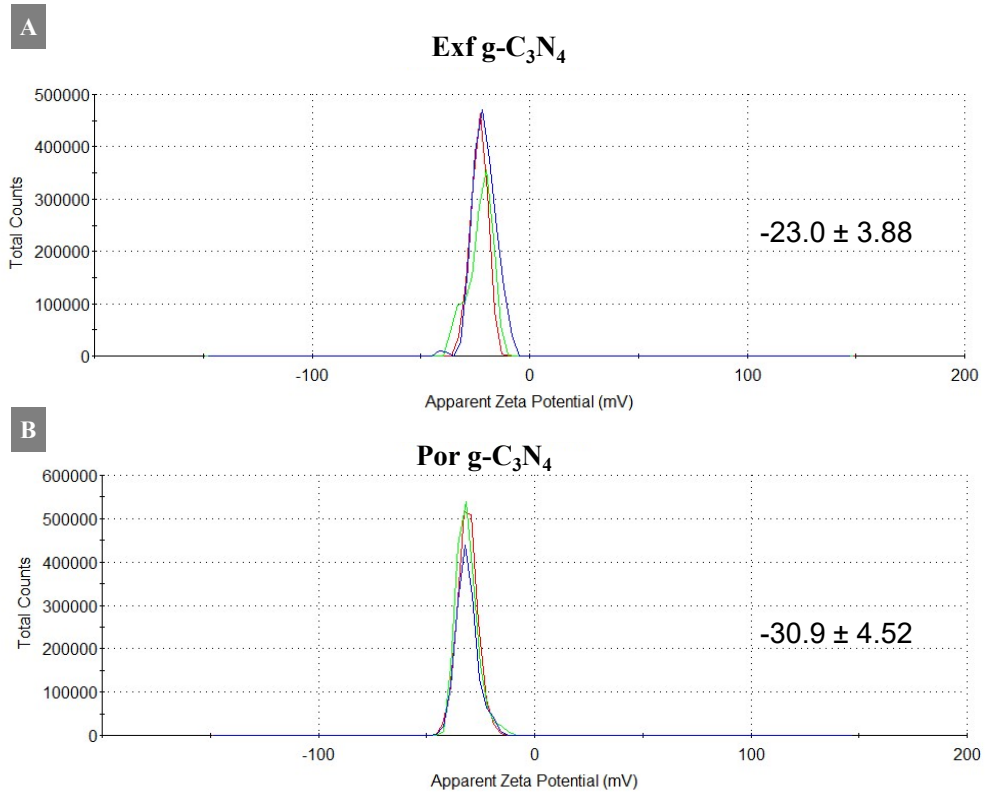


**Figure S3:** Zeta potential of the synthesized Exf and Por g-$C_3N_4$ nanosheets.

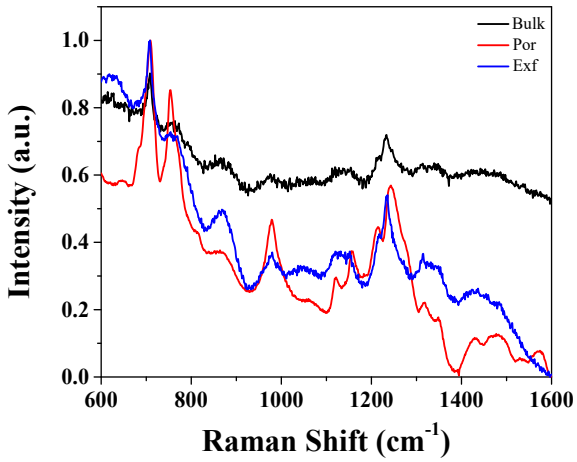


Vibration modes of C-N heterocycles ($cm^{-1}$):

- 708, 978 : Breathing mode of triazine.
- 754 : Out-of-plane bending mode (porous).
- 1234: N=C $sp^2$ bending vibration.
- 1257: O-H in-plane bending mode in COOH.
- 1574: N-C-N symmetric stretching.

**Figure S4:** Raman spectra of the synthesized Exf and Por g-$C_3N_4$ nanosheets.

Raman spectroscopy was employed to get better insights into the structure of Por and Exf sheets (**Fig. S4**). The characteristic peaks of CN heterocycles vibration modes are 708, 978, 754, 1234, 1257, and 1575 $cm^{-1}$. The peaks at 708 and 978 $cm^{-1}$ constituted the breathing modes of the triazine ring. The out-of-plane bending mode of the graphitic domain was observed at 754 $cm^{-1}$. The similarity in the Raman spectra of Exf to bulk g-$C_3N_4$ was attributed to preserving the same crystal structure.[1] However, in Por g-$C_3N_4$, the peak at 1234 $cm^{-1}$ is highly blue shifted and broadened at 1249 $cm^{-1}$, corresponding to very thin sheets, and the defect like C-OH: (1257 $cm^{-1}$ is the OH in-plane bending mode in C-OH).[9]

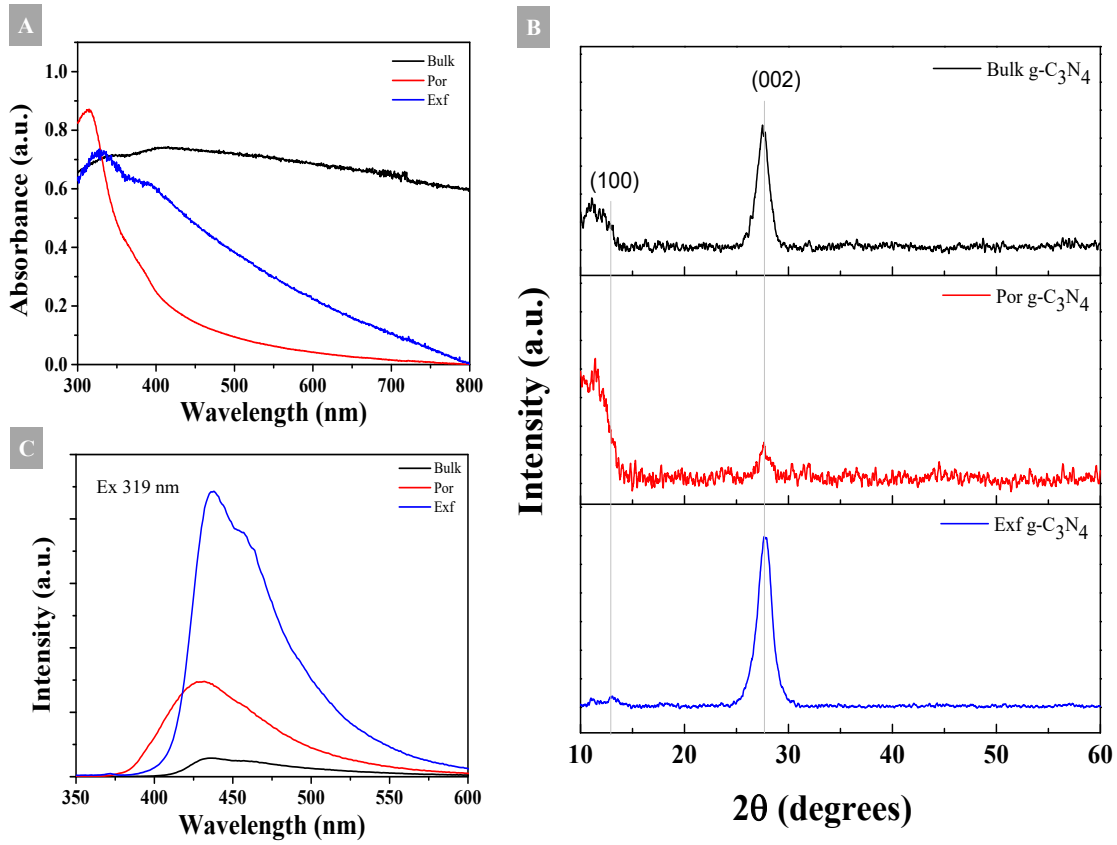


**Figure S5: (A)** Absorption spectra, **(B)** XRD pattern and **(C)** fluorescence spectra of bulk, Exf and Por g-$C_3N_4$ as denoted in the graphs.

The UV-vis spectra (**Fig. S5A**) showed the characteristic absorbance peaks of Exf and Por nanosheets at 330 nm and 315 nm respectively. The bulk g-$C_3N_4$ has a broad absorbance band edge around 450 nm. The slight blue shift of both Exf and Por g-$C_3N_4$ compared to bulk g-$C_3N_4$ can be attributed to the increased band gap between the valence and conduction band[10] due to the quantum confinement effect as the bulk material forms ultrathin sheets of exfoliated and porous g-$C_3N_4$.[2]

Further, the fluorescence of the Exf and Por g-$C_3N_4$ nanosheets was observed under the excitation at 318 nm. **Fig. S5B** showed the photoluminescence spectra of Exf and Por g-$C_3N_4$ nanosheets wherein a slight blue shift was shown by Por g-$C_3N_4$ nanosheets due to the decreased conjugation length and the quantum confinement effect.[11, 12]
The x-ray diffraction pattern (**Fig. S5C**) of bulk g-$C_3N_4$ had two major peaks (002 plane) at 13° and 27.4°. The peak at 27.4° could be correlated to the π-conjugation in the stacks of interlayers of tris-s-triazine rings while the peak at 13° corresponded to the intralayer packing pattern.[13] The Exf g-$C_3N_4$ showed only one peak at 27°, which implied the z-plane was in good orientation with the xy-plane.[1, 14] The decrease in the overall intensity is observed at 27° for Por g-$C_3N_4$ nanosheets, which could be attributed to the effect on the geometric confinement due to the porous microstructure.[2]

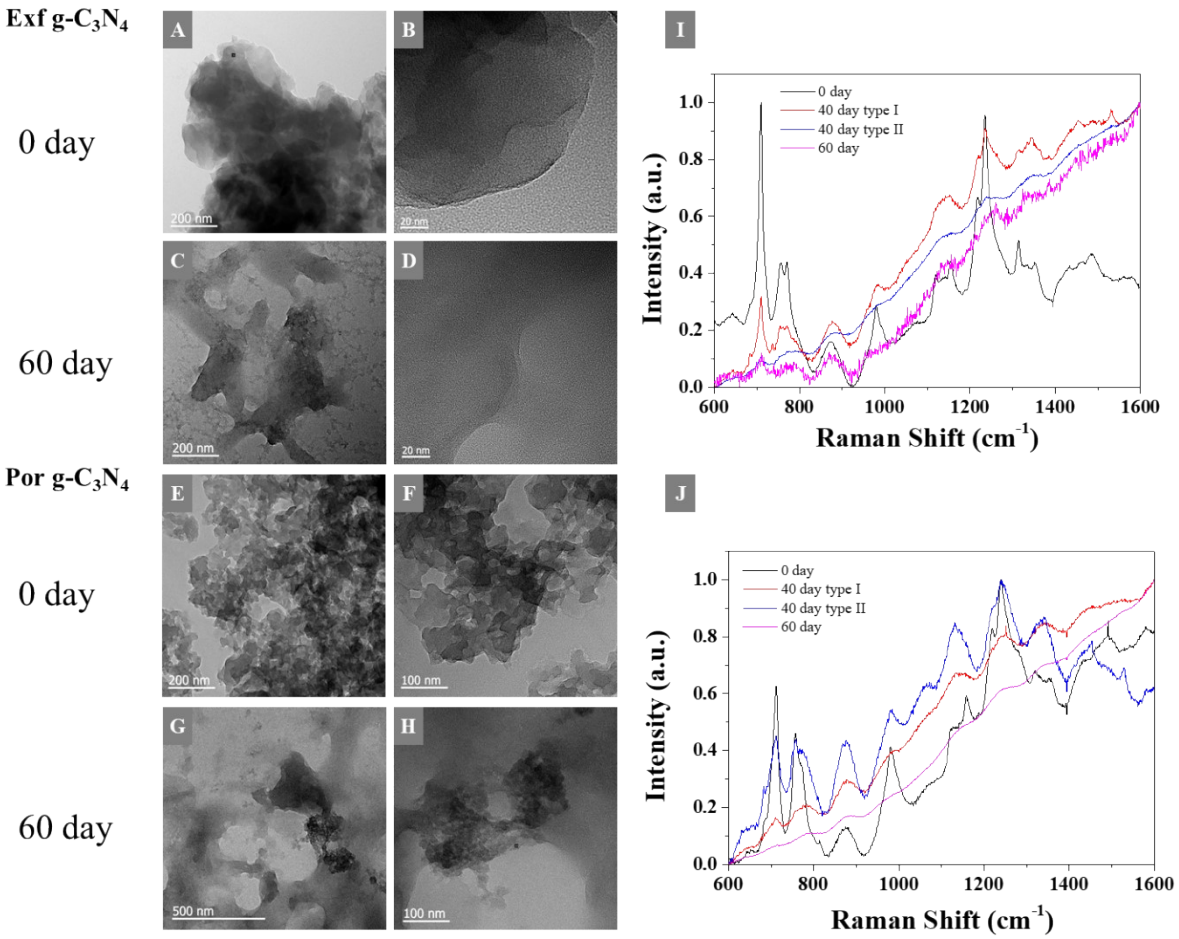


**Figure S6:** TEM analyses of Exf 0-day (A and B) and 60 days (C and D) along with Por 0-day (E and F) and 60 days (G and H) g-$C_3N_4$ sheets after degradation using HRP. Raman spectroscopic analyses of Exf (I) and Por (J) g-$C_3N_4$ sheets (0- and 60-day samples).

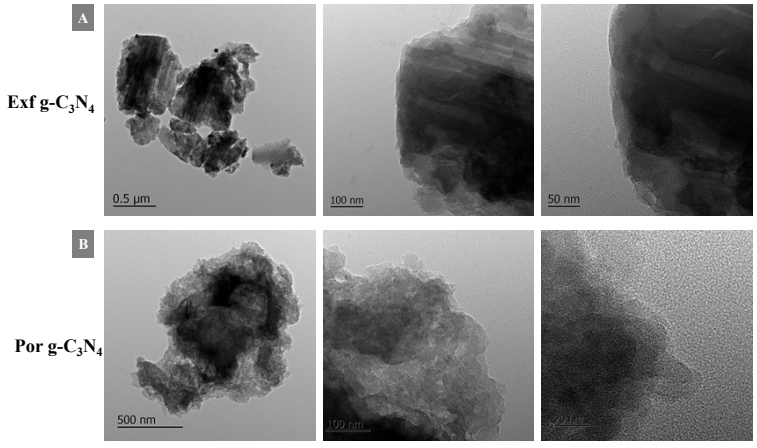


**Figure S7:** TEM analyses of Exf (A) and Por (B) g-$C_3N_4$ sheets after 150 hr treatment with $H_2O_2$ alone as control samples for degradation via PF reaction.

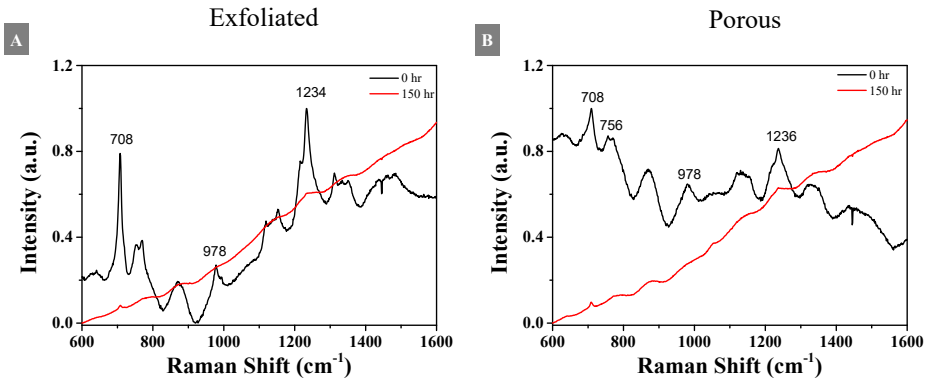


**Figure S8:** Raman spectroscopic analyses of Exf and Por g-$C_3N_4$ nanosheets after PF reaction for 150 hr compared with 0 hr control samples.

**Table S1**: The percentage of C, N and O in exfoliated and porous g-$C_3N_4$ at 0 hr and 150 hr after PF reaction analysed using XPS survey spectra.

| | Exf 0 hr | Exf 150 hr | Por 0 hr | Por 150 hr |
|---|---|---|---|---|
| C % | 50.48 | 38.82 | 35.17 | 60.01 |
| N % | 46.81 | 6.25 | 51.89 | 1.51 |
| O % | 2.72 | 54.93 | 12.94 | 38.48 |

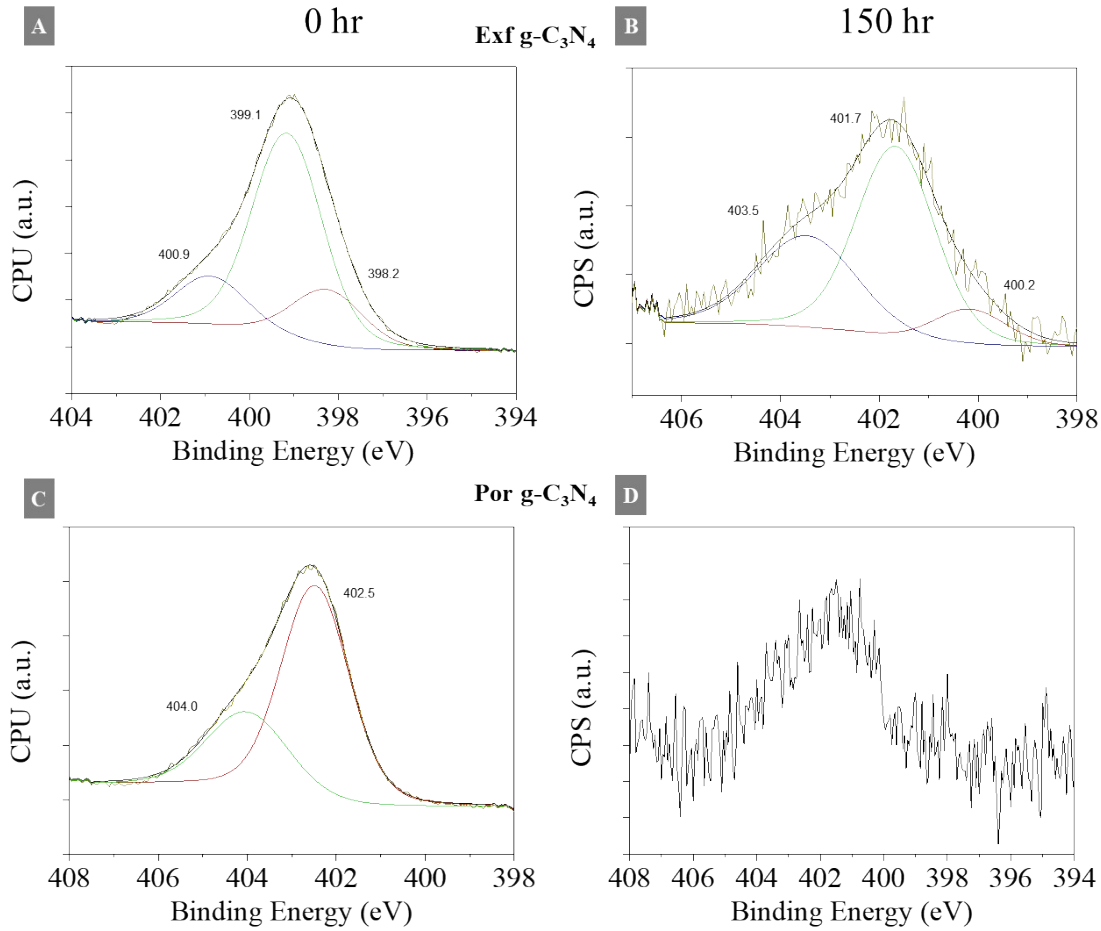


**Figure S9:** Deconvoluted spectra of N1s for Exf and Por g-$C_3N_4$ nanosheets before (A and C, respectively) and after degradation using PF reaction for 150 hr (B and D, respectively).

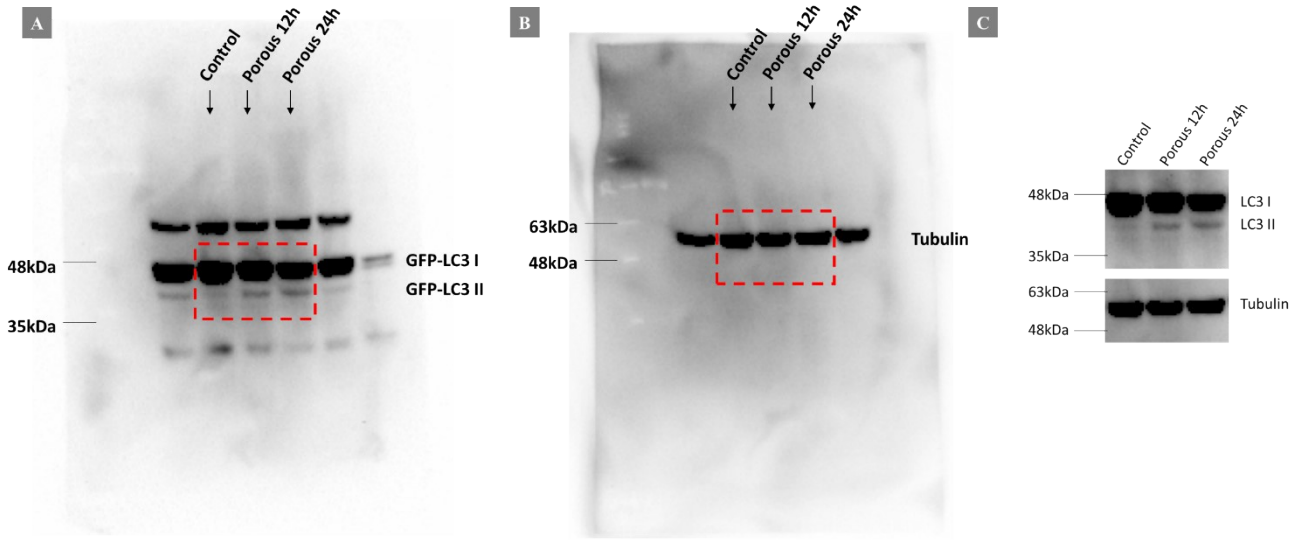


**Figure S10.** Raw data for the full-length western blots in Fig.6D: Probed for (A) GFP-LC3, and (B) Tubulin. The red box represents the depicted lanes of the blot. The membrane was first probed for tubulin, then stripped and re-probed for GFP. (C) The cropped image of the western blot data as shown in Fig. 6D.

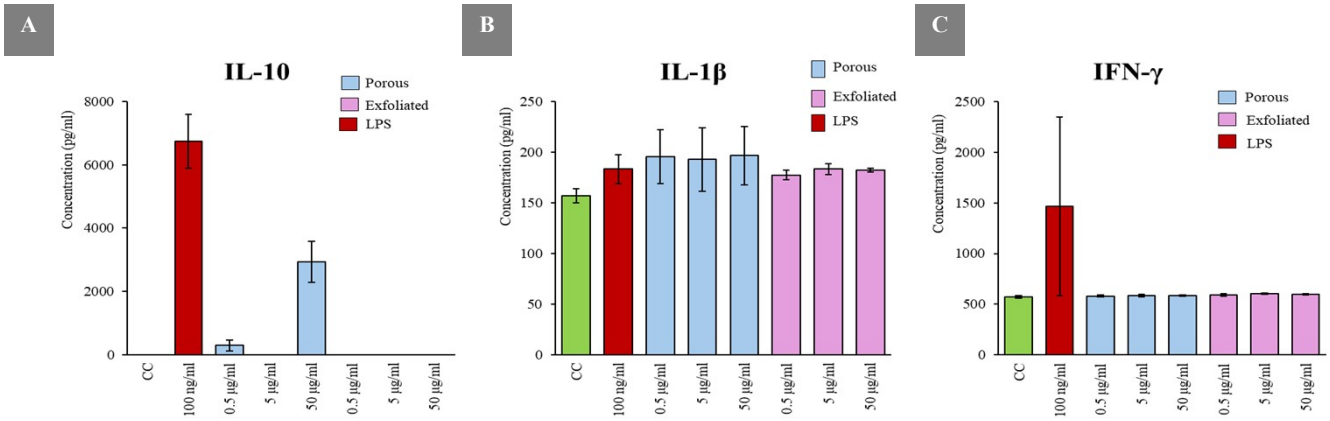


**Figure S11:** (A) IL-10 cytokines were estimated by sandwich ELISA method. The effect of Exf and Por g-$C_3N_4$ nanosheets on IL-1β and IFN-γ: RAW 264.7 Macrophages were treated with nanomaterials at 0.5 µg/mL, 5 µg/mL, and 50 µg/ml concentrations for 24 hr. (B) IL-1β and (C) IFN-γ cytokines were estimated by sandwich ELISA method.

## References


1. Zhang, X.; Xie, X.; Wang, H.; Zhang, J.; Pan, B.; Xie, Y., Enhanced Photoresponsive Ultrathin Graphitic-Phase C3N4 Nanosheets for Bioimaging. *Journal of the American Chemical Society* **2013,** *135* (1), 18-21.

2. Li, H.-J.; Sun, B.-W.; Sui, L.; Qian, D.-J.; Chen, M., Preparation of water-dispersible porous g-C3N4 with improved photocatalytic activity by chemical oxidation. *Physical Chemistry Chemical Physics* **2015,** *17* (5), 3309-3315.

3. Kurapati, R.; Russier, J.; Squillaci, M. A.; Treossi, E.; Ménard-Moyon, C.; Del Rio-Castillo, A. E.; Vazquez, E.; Samorì, P.; Palermo, V.; Bianco, A., Dispersibility-Dependent Biodegradation of Graphene Oxide by Myeloperoxidase. *Small (Weinheim an der Bergstrasse, Germany)* **2015,** *11* (32), 3985-3994.

4. Rajendra, K.; Fanny, B.; Julie, R.; Adukamparai Rajukrishnan, S.; Cécilia, M.-M.; Kostas, K.; Alberto, B., Covalent chemical functionalization enhances the biodegradation of graphene oxide. *2D Materials* **2018,** *5* (1), 015020.

5. Bai, H.; Jiang, W.; Kotchey, G. P.; Saidi, W. A.; Bythell, B. J.; Jarvis, J. M.; Marshall, A. G.; Robinson, R. A. S.; Star, A., Insight into the mechanism of graphene oxide degradation via the photo-fenton reaction. *Journal of Physical Chemistry C* **2014,** *118* (19), 10519-10529.

6. Swetha, K.; Camisasca, A.; Bartkowski, M.; Garhwal, A.; Aravind, A.; Gnanadhas, P.; Giordani, S.; Kurapati, R., Biodegradability of Carbon Nano-Onions by Human Myeloperoxidase and Photo-Fenton Process. *ChemNanoMat* **2024,** *10* (6), e202300630.

7. Karki, R.; Park, C.-H.; Kim, D.-W., Extract of buckwheat sprouts scavenges oxidation and inhibits pro-inflammatory mediators in lipopolysaccharide-stimulated macrophages (RAW264.7). *Journal of Integrative Medicine* **2013,** *11* (4), 246-252.

8. Reddy Bonam, S.; Naidu Gorantla, J.; Thangarasu, A. K.; Lankalapalli, R. S.; Sampath Kumar, H. M., Polyhydroxy-N-alkyl-2-pyrrolidinones as a new class of glycolipid analogues with immune modulation potential. *Journal of Carbohydrate Chemistry* **2018,** *37* (1), 30-43.

9. Bai, Y.; Chen, M.; Liu, Y.; Zhou, Y.; Gan, D.; Tu, W., Self-assembly of porous g-C3N4 and montmorillonite: characterization, performance test, and mechanism analysis. *Journal of Materials Science: Materials in Electronics* **2022,** *33* (7), 3631-3647.

10. Zhang, S.; Thuy Hang, N.; Zhang, Z.-J.; Yue, H.; Yang, W., Preparation of g-C3N4/Graphene Composite for Detecting NO2 at Room Temperature. *Nanomaterials* **2017,** *7*, 12.

11. Kim, K.; Park, Y.-G.; Hyun, B. G.; Choi, M.; Park, J.-U., Recent Advances in Transparent Electronics with Stretchable Forms. **2019,** *31* (20), 1804690.

12. Xu, J.; Zhang, L.; Shi, R.; Zhu, Y., Chemical exfoliation of graphitic carbon nitride for efficient heterogeneous photocatalysis. *Journal of Materials Chemistry A* **2013,** *1* (46), 14766-14772.

13. Tian, J.; Liu, Q.; Ge, C.; Xing, Z.; Asiri, A. M.; Al-Youbi, A. O.; Sun, X., Ultrathin graphitic carbon nitride nanosheets: a low-cost, green, and highly efficient electrocatalyst toward the reduction of hydrogen peroxide and its glucose biosensing application. *Nanoscale* **2013,** *5* (19), 8921-8924.

14. Wang, X.; Maeda, K.; Thomas, A.; Takanabe, K.; Xin, G.; Carlsson, J. M.; Domen, K.; Antonietti, M., A metal-free polymeric photocatalyst for hydrogen production from water under visible light. *Nature materials* **2009,** *8* (1), 76-80.